Energy 103 (2016) 369–384

Contents lists available at ScienceDirect

Energy

journal homepage: www.elsevier.com/locate/energy

# Transient natural gas liquefaction and its application to CCC-ES (energy storage with cryogenic carbon capture™)

Farhad Fazlollahi*, Alex Bown, Edris Ebrahimzadeh, Larry L. Baxter**

*Chemical Engineering Department, Brigham Young University, Provo, UT 84602, USA*

ARTICLE INFO

*Article history:*
Received 19 April 2015
Received in revised form
23 November 2015
Accepted 18 February 2016
Available online 25 March 2016

*Keywords:*
Transient natural gas liquefaction
Optimization
Exergy analysis
Aspen HYSYS

ABSTRACT

This paper presents steady-state and transient models and optimization of natural gas liquefaction using Aspen HYSYS. Steady-state exergy and heat exchanger efficiency analyses summarize the performance of several potential systems. Transient analyses of the optimal steady-state model produced most of the results discussed here. These results pertain to LNG (liquefied natural gas) generally and to an energy storage process associated with CCC (cryogenic carbon capture™) in which the LNG process plays a prominent role specifically. The energy storage CCC process influences the time constants and magnitudes of the flow rate characteristics. These flowrate variations affect all units, especially compressors and heat exchangers. The proposed process controls temperatures, pressures and other operating parameters. K-value- and U-value-techniques guide flowrate and heat exchanger stream variations. Transient responses to both ramping and step-changes in flow rates indicate process responses, including summary effects represented in transient efficiency graphs.



## 1. Introduction

Global economic development and population expansion increase energy demand and stress energy supply systems [1]. The focus of this paper is on energy primarily in the forms of electrical power from fossil-fuel power plants and the fuels that fire them. One of the most critical needs of energy supply systems is energy storage. Energy storage is the conversion of energy from an easily usable form that is hard or expensive to store to a different form that stores more conveniently or economically and, typically at a later time, back to the original or to another easily usable form. The most desirable characteristics of energy storage systems are rapid response to changes in demand; high round-trip efficiency; and low cost.

The LNG (liquefied natural gas) process is well represented in the literature [2–5]. The efficiency and capital cost for these processes are well known and the differences are typically small with regard to thermodynamics. The real keys in developing a successful liquefaction plant are equipment selection and its configurations to meet a plant's capacity goals. Remeljej et al. [6] showed that a single-stage mixed refrigerant cycle had the lowest exergy losses. Melaaen simulated the natural gas liquefaction process of a base load plant by DASSL [7]. Gu An-zhongs research group [7] also simulated natural gas liquefaction processes. Cao et al. [8] optimized power consumption of NG (natural gas) liquefaction processes using a mixed refrigerant cycle and HYSYS and concluded that an $N_2$–$CH_4$ expander cycle requires lower power consumption in the compression stages. Mowla and Mokarizadeh [9] optimized a SMR (single mixed refrigerant) cycle using MATLAB and a GA (genetic algorithm) to generate the objective function. Kikkawa [10] designed the pre-cooling mixed-refrigerant cycle and expander cycle, and analyzed them with CHEMCAD while Van de Graaf and Pek [11] claims the Shell PMR (parallel mixed refrigerant) process is more efficient.

This paper provides transient analyses of LNG production processes that with the results discussed in this previously cited literature. The motivation for this work is to produce LNG used in a carbon capture process called CCC (cryogenic carbon capture™). The following discussion outlines the role of LNG production in CCC, after which this paper presents the detailed discussion of the analyses and results.

* Corresponding author.
** Corresponding author.
*E-mail addresses:* farhad.fazlollahi@gmail.com, Farhad@byu.edu (F. Fazlollahi), Larry_baxter@byu.edu (L.L. Baxter).

http://dx.doi.org/10.1016/j.energy.2016.02.109
0360-5442/

**Nomenclature**

*Parameters and variables*

| | |
|---|---|
| a | the attractive parameter [Pa($m^3$/mole)$^2$] |
| A | dimensionless attractive parameter |
| b | the effective molecular volume [$m^3$/mole] |
| B | dimensionless effective molecular volume in Peng–Robinson equation of state |
| E | exergy [kW] |
| $\Delta E_x$ | exergy losses of the equipment [kW] |
| $E_{in}$ | inlet exergy of the equipment [kW] |
| $E_{out}$ | outlet exergy of the equipment [kW] |
| $g_i$ | Gibbs energy of stream i [kJ/kg] |
| $\widehat{g}_i$ | specific Gibbs energy of stream i [kJ/kg] |
| $\widehat{h}_i$ | specific enthalpy of stream i [kJ/kg] |
| $H_0$ | enthalpy at ambient temperature [kJ] |
| $H_{in}$ | inlet enthalpy of the equipment [kJ] |
| $H_{out}$ | outlet enthalpy of the equipment [kJ] |
| k | pressure flow coefficient $\left[\frac{kg}{h}\times\sqrt{\frac{\frac{kg}{m^3}}{kPa}}\right]$ |
| $k_{ij}$ | binary interaction coefficient |
| $m_i$ | mass flow rate of stream i [kg/h] |
| P | pressure [kPa] |
| $\Delta P$ | total pressure drop [kPa] |
| $q_{LNG}$ | mass flow of the produced LNG [kg NG] |
| R | universal gas constant |
| S | entropy [kJ/K] |
| $S_i$ | entropy of stream in efficiency equation [kJ/K] |
| $\widehat{s}_i$ | specific entropy of stream i [kJ/kg K] |
| $S_0$ | entropy at ambient temperature [kJ/K] |
| $S_{in}$ | inlet entropy of the equipment [kJ/K] |
| $S_{out}$ | outlet entropy of the equipment [kJ/K] |
| T | temperature [K] |
| t | temperature [°C] |
| $T_i$ | temperature of stream i [K] |
| $T_0$ | ambient temperature [K] |
| $Tw_{in}$ | temperature of water into the water cooler [K] |
| $Tw_{out}$ | temperature of water out of the water cooler [K] |
| UA | overall heat transfer coefficient [kJ/°C h] |
| V | volume [$m^3$] |
| $v$ | molar volume [$m^3$/mole] |
| W | power [kW] |
| $W_c$ | power consumption of the compressor [kW] |
| $W_e$ | power consumption of the expander [kW] |
| Z | compression factor |
| $z_i$ | mole fraction for the component of i |
| $z_j$ | mole fraction for the component of j |
| $\eta$ | heat exchanger's efficiency |
| $\rho$ | density [$kg/m^3$] |

*Acronyms*

| | |
|---|---|
| B | balanced case |
| CCC | cryogenic carbon capture™ |
| ER | energy recovery case |
| ES | energy storage case |
| LNG | liquefied natural gas |
| MITA | minimum internal temperature approach |
| MR | mixed refrigerant |
| NG | natural gas |
| PR | Peng–Robinson equation of state |
| SMR | single mixed refrigerant |

## 2. Features of cryogenic carbon capture™

CCC (cryogenic carbon capture™) provides cost-effective and energy-efficient $CO_2$ separation from flue gases compared to the alternative technologies [12–14]. One version of CCC also provides highly efficient, rapidly responding, very inexpensive energy storage. This energy storing version of CCC consists of two major subsystems: the traditional cryogenic carbon capture™ system and energy storage via natural gas liquefaction. The natural gas liquefaction functions as a refrigerant for CCC [14].

Surges in power supply and demand arise from: (1) typical daily patterns of high-energy demand during the afternoon and low demands in the night, (2) intermittent contributions from renewables such as wind or solar energy, and (3) grid instabilities. These changes in supply typically drive changes in average energy production cost and energy price in addition to several more

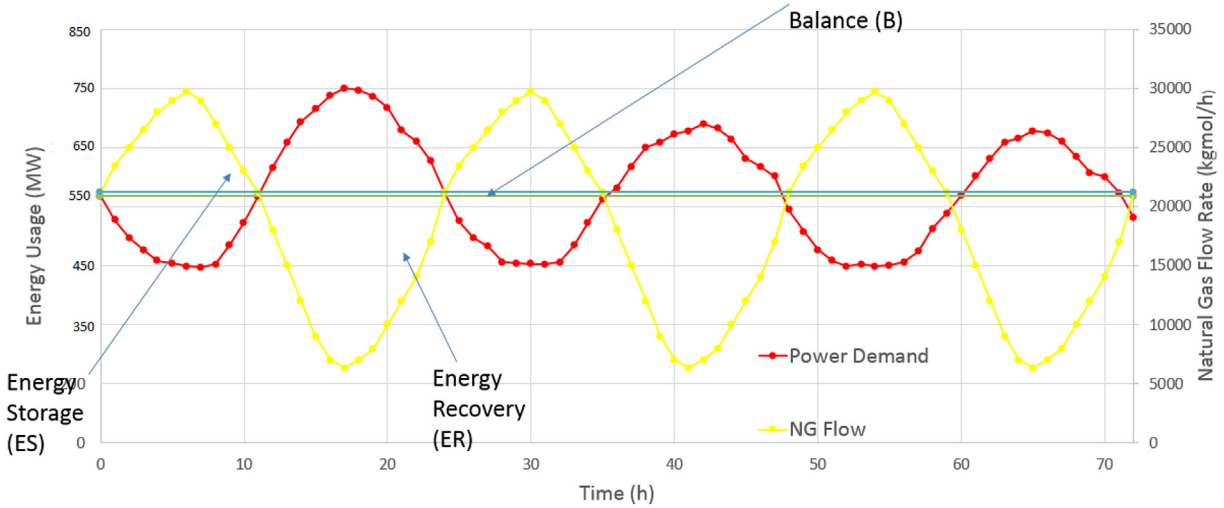


**Fig. 1.** Typical power plant and system demand patterns in three cases.

**Table 1**
Mole fractions of the feed gas and other parameters in the process.

| Parameters | Value | | Notes |
|---|---|---|---|
| Feed gas pressure | 3700 kPa | | |
| Feed gas temperature | 21 °C | | |
| Feed gas flow rate | 21,200 kgmol/h | | |
| Feed gas mole fraction components | $CH_4$ | 0.95 | |
| | $C_2H_6$ | 0.03 | |
| | $C_3H_8$ | 0.02 | |
| LNG storage pressure | 1145 kPa | | |
| LNG temperature before expansion | −94 °C | | |
| NG temperature after expansion | −119.4 °C | | |
| Pressure drop in heat exchanger | 5 kPa | | To simplify the process |
| Pressure drop in water cooler | 1 kPa | | |
| Temperature after water cooler | 21 °C | | |
| Ambient temperature | 25 °C | | |
| The adiabatic efficiency of compressor | 92% | | [14,18] |
| The adiabatic efficiency of turbine | 92% | | [14,18] |
| Pressure ratio of each compressor | 1–3 | | |
| Water's temperature from CCC | 1.0561 °C | | |
| From CCC's temperature | −98.5 °C | | |
| The minimum approach temperature of heat exchanger | 1–3 °C | | |

**Table 2**
Basic condition for model.

| Conditions | From pipeline | To CCC (final conditions) |
|---|---|---|
| Vapor/phase fraction | 1 | 0.27 |
| Temperature [°C] | 21 | −119.4 |
| Pressure [kPa] | 3700 | 1145 |

complicated and region-specific issues. Such large cost swings generally cause technical and economic mischief on the grid. CCC mitigates these problems, dramatically increasing grid and price stability over a period of one or several days, using an energy storage system as explained here. The CCC process can use natural gas as a refrigerant. This refrigerant provides very high-energy storage density, with the energy required for both the temperature and phase change stored in the LNG. Once liquefied, the liquid natural gas storage loses less than 0.05% over multiple days [15]. The energy-storing version of CCC stores surges in energy supply or periods of low energy cost by liquefying more natural gas than is needed at the time of the surge or low cost. This excess production terminates when the surge in supply of drop in costs returns to normal. During high-energy demand or expensive energy production periods, the cryogenic carbon capture™ process operates on stored liquefied natural gas, reducing its parasitic load dramatically and thereby increasing the amount of net energy produced by the power plant. Current commercial LNG storage technologies easily allow for many hours of energy storage for even the largest coal-fired power plants by this technique. In practical applications, the energy storage rate of this process typically could be up to 50% of the power plant capacity while the rate of energy release could be about 15% of the plant capacity.

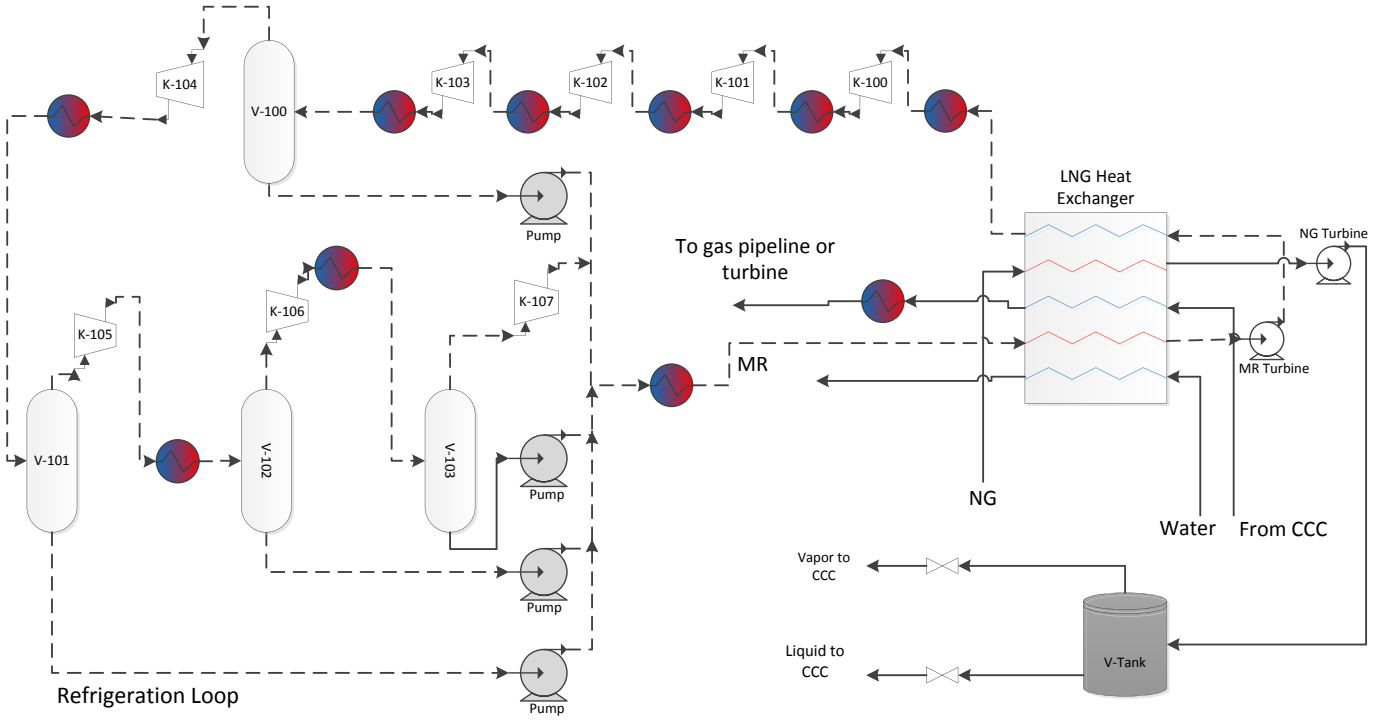


**Fig. 2.** HYSYS simulation of SMR.

**Table 3**
Mixed refrigerant conditions and key parameters for three cases.

| Conditions | Entrance | | | Loop | | |
|---|---|---|---|---|---|---|
| | ER | B | ES | ER | B | ES |
| Vapor/phase fraction | 0.43 | 0.023 | 0.00 | 0.230 | 0.086 | 0.100 |
| Temperature [°C] | 30.00 | 20.5 | 16.12 | −87.99 | −93.191 | −92.05 |
| Pressure [kPa] | 3704.65 | 3704.65 | 3704.65 | 108.4 | 108.394 | 108.40 |

| Component | Mole fraction |
|---|---|
| Methane | 0.0423 |
| Ethane | 0.8451 |
| Propane | 0.0000 |
| n-Butane | 0.02813 |
| n-Pentane | 0.08447 |

However, the rate of energy release could be much higher, as explained next.

The open refrigeration loop could either return the warm natural gas to the pipeline or feed a gas turbine. The fastest response to fluctuating demand in power generation occurs with simple cycle gas turbines [16]. Simple cycle turbines do not recover heat from the flue gas because it would interfere with response speed. With ES-CCC, the natural gas could burn in a simple cycle turbine, increasing the effective amount of energy returned to the grid. However, because the turbine would be adjacent to a standing coal or combined-cycle natural gas facility with a Rankine-cycle boiler, the effluent from this turbine could feed the boiler, allowing combined cycle efficiency at simple cycle cost. In this way, the cryogenic carbon capture™ system can both dramatically reduce $CO_2$ emissions from fossil plants and significantly increase the effectiveness of intermittent renewables to overall power supply.

Since a plant must eliminate $CO_2$ emissions; this added capacity from the natural gas combustion is a powerful way to justify a portion of the equipment costs. Although $CO_2$ removal can have significant costs, the energy storage system leverages the capital already installed for efficiency and allows higher penetration for renewable energy sources because of improved ramping capabilities. This time shifting or demand response enables a form of energy storage that is very large scale, highly efficient, and very cost effective. This paper demonstrates that it can also be rapidly responding.

The $CO_2$ removal process requires a constant source of refrigerant. When this refrigerant supply meets the CCC demand, the process is balanced (B). Excess LNG used as a refrigerant to drive

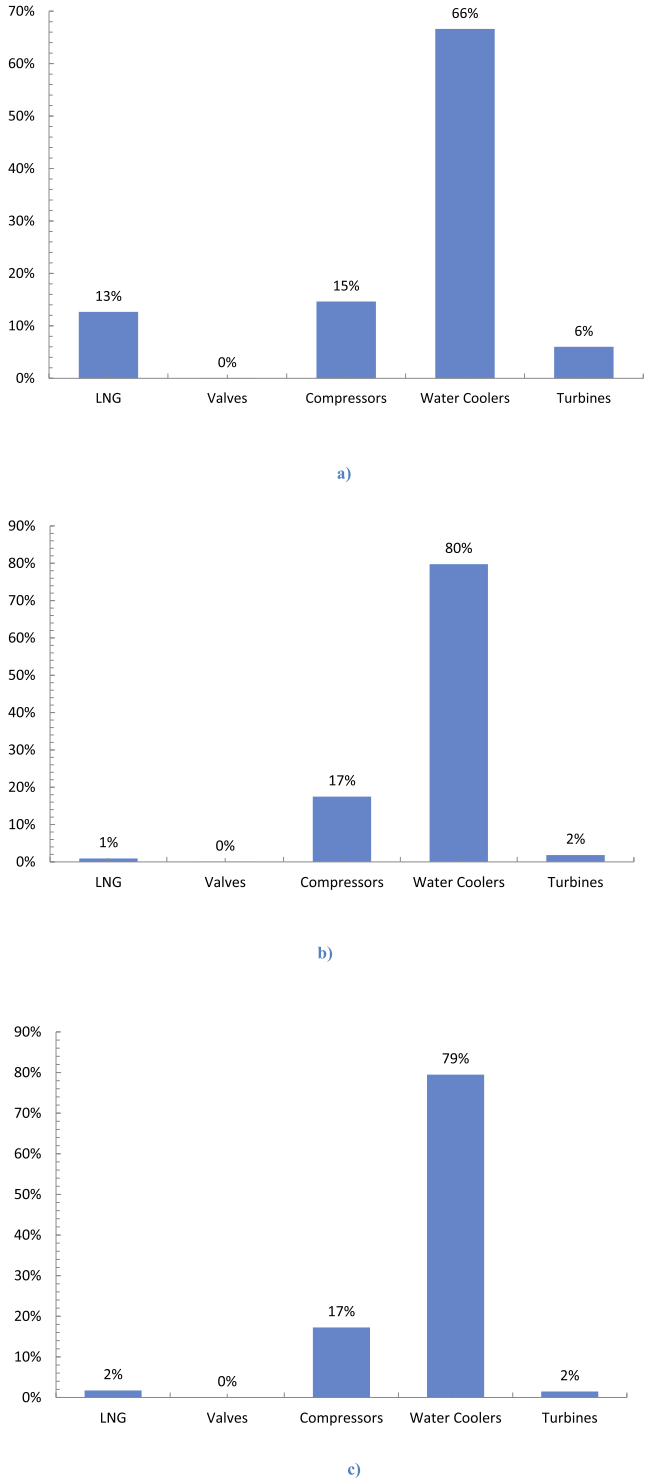


**Fig. 3.** Major equipment exergy losses in a) ER, b) B and c) ES.

**Table 4**
Optimized energy input requirements for each case.

| | ER | B | ES |
|---|---|---|---|
| Energy input requirements (kW/kg NG) | 0.0083 | 0.0613 | 0.0706 |

**Table 5**
Exergy change expressions for differing types of equipment.

| Equipment | Exergy loss equation |
|---|---|
| Compressor | $\Delta E_x = E_{in} - E_{out} + W_c$ |
| Expander | $\Delta E_x = E_{in} - E_{out} - W_c$ |
| LNG heat exchanger | $\Delta E_x = \sum E_{in} - \sum E_{out}$ |
| Water cooler | $\Delta E_x = E_{in} - E_{out}$ |
| Valve | $\Delta E_x = T_0(S_{out} - S_{in})$ |

**Table 6**
Total exergy loss for three cases.

| | ER | B | ES |
|---|---|---|---|
| Exergy loss (kW) | 970 | 13,630 | 25,840 |

**Table 7**
Heat exchanger's efficiency for each case.

| | ER (%) | B (%) | ES (%) |
|---|---|---|---|
| Heat exchanger's efficiency | 74.35 | 93.86 | 80.21 |

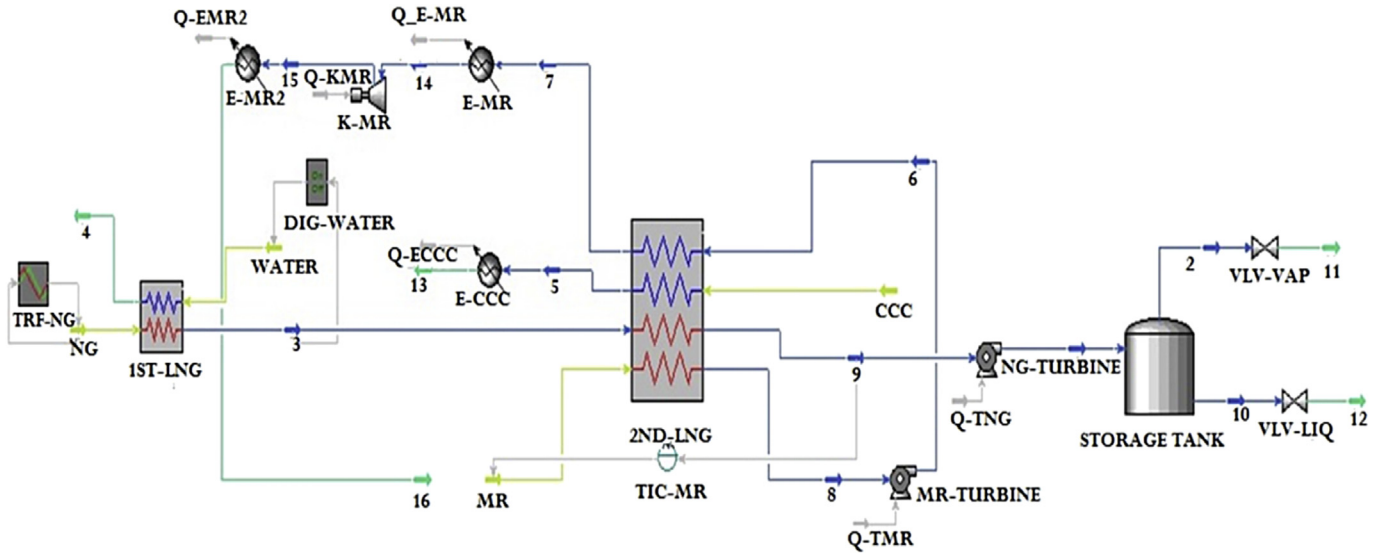


**Fig. 4.** Transient modeling of SMR liquefaction process.

the system can be stored for further use. During off peak hours, this ES (energy-storing) version of the process generates more refrigerant in the compressors than is needed for the process and the excess refrigerant is stored in an insulated vessel as a low-temperature liquid at a modest-pressure. During peak demand, the previously stored energy in the form of the stored, condensed refrigerant provides ER (energy recovery) by replacing the compressor energy with the stored refrigerant, eliminating nearly all of the energy demand required by cryogenic carbon capture™ for as long as the stored refrigerant lasts. Fig. 1 illustrates typical daily variations in power supply and the potential regions of energy storage and energy recovery. In this particular case, the balanced operation occurs only during the transition between recovery and storage. The horizontal line is the average energy production and demand. This paper develops and discusses the transient model which could satisfy this pattern while consuming minimum energy.

The LNG process used in CCC differs from the analyses briefly reviewed in the introduction in that it always incorporates a return NG stream, similar to ASU (air separation unit) processes that incorporate substantial recuperative heat exchange. The traditional processes produce and deliver LNG, typically with little or no return stream through the production cycle. The CCC process uses LNG as a refrigerant and, in fact, primarily uses only refrigeration associated with LNG vaporization. Therefore, the LNG process analyzed here benefits from significant heat integration, warming low-pressure LNG vapor returning from the CCC process by cooling high-pressure LNG streams entering the process. This heat integration results in LNG production at notably lower energy and economic costs compared to traditional systems when the system operates in either energy recovery or balanced modes. Nevertheless, the process is similar enough to traditional processes that the substantial commercial experience and published analyses remain germane to this process, with some modification. This investigation applies the results of the previous investigations to this somewhat different process to analyze a system that has aspects in common with traditional LNG and ASU processes. However, the transient analysis developed here has very little precedent in the literature. It is crucial to reduce entropy generation due to temperature difference between feed natural gas and return refrigerant flows in the LNG heat exchangers. Large temperature differences and heat exchange load are the primary reasons of exergy loss in heat exchangers. Additionally, the LNG process here uses staged compression with intercooling [17].

Aside from the return flows making these LNG processes unique compared to traditional analyses, this investigation focuses on transient modeling. Although there are many publications on the steady-state design and optimization of NG liquefaction processes, there are few transient models with natural gas flow variation. Several studies have focused on optimization and steady state modeling with few if any addressing the optimality of this process in transient mode and from a process control perspective. Liquefied natural gas plant design is based on steady-state process simulation. The use of a dynamic process simulator provides insight to actual plant transients and dynamics, verifies control schemes, and highlights plant safety procedures. The dynamic model calculates process variables as functions of time. Moreover, it is possible to examine process upsets, including process startups and shutdowns – critical information not offered by steady-state simulations. Dynamic simulation can explore the entire range of plant conditions and the issues associated with startup, load changes, upsets, and shutdown. Dynamic simulation enables engineering analysts to evaluate design modifications and to capture cases where the original design was not satisfactory for startup. The need for transient modeling also addresses feed stream changes with time. In this investigation, Aspen HYSYS Dynamics provides the transient modeling of LNG production. The simulator controls temperatures, pressures and other operating conditions. K-value and U value techniques provide control mechanisms for heat exchangers. Mixed refrigerant and natural gas flowrates vary with time. Process and heat exchanger efficiencies graphs summarize temporal process responses to changing flows.

## 3. Materials and methods

### 3.1. Process design

#### 3.1.1. Feed gas parameters

The simulations discussed in this paper require several specifications as summarized in Table 1. A feed gas flow rate of 21,200 kgmol/h is required for the steady operation of CCC on a 550 MW net output power plant. During energy storage and recovery, the rates change to 29,680 kgmol/h and 6360 kgmol/h, respectively. These flow rates represent a 40% increase and a 70%

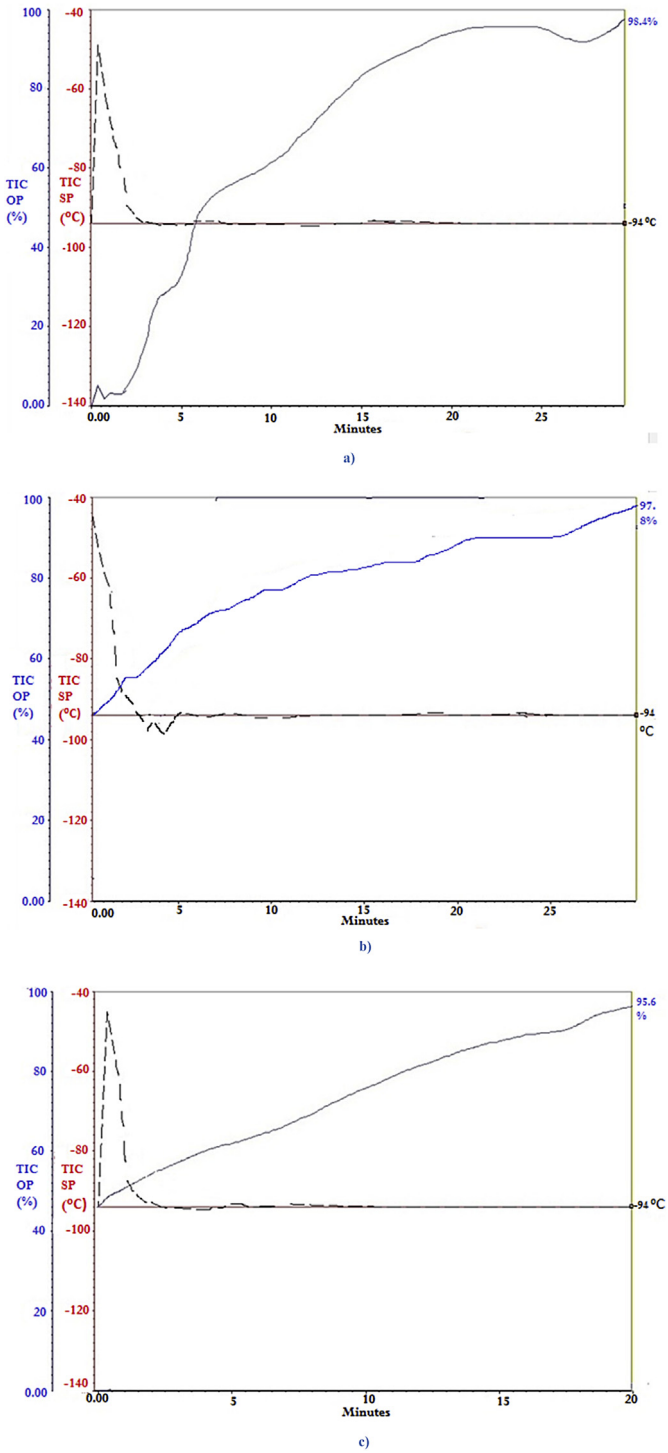


**Fig. 5.** PID controller in the a) B, b) ES and c) ER cases, solid red line = set point °C; dashed black line = temperature °C.

decrease in coolant flow compared to the steady-state demand. The assumption here is that the amount of cooling provided to the CCC process at the power plant is constant (base-loaded plant) while the demand on power for the LNG production process could change +40% to −70% based on grid variations. In reality, the off-peak demand commonly lasts much longer than the peak demand, so the increase in LNG flow could be much smaller than even these numbers reflect compared to a potential large decrease in flow. All other parameters mentioned in Table 2 remain constant. The liquefaction rate is 100% after the main heat exchanger, but to satisfy our purposes in the CCC process (to avoid temperature cross in CCC's heat exchanger, output temperature of LNG plant should be around −120 °C), the LNG partially vaporizes (27%) after the main heat exchanger.

### 3.2. Liquefaction process-SMR (single mixed refrigerant) cycle

The SMR is the simplest NG liquefaction process. The Single MR (mixed refrigerant) Cycle uses only one MR loop for pre-cooling, liquefaction, and sub-cooling (Fig. 2). The cycle compresses and cools the refrigerant until liquid is formed, and then vaporizes the refrigerant in the LNG exchanger. The refrigerant cools and condenses the natural gas to liquefied natural gas, LNG. The refrigerant composition maintains the temperature profiles in the heat exchangers as close and parallel as possible.

The simulation flow sheet of the SMR process (Fig. 2) uses an eight-stage compressor with inter-stage cooling. Phase separators separate the mixed refrigerant into gas and liquid phases in each cooler. Pumps compress the liquid after the phase separator. A single LNG heat exchanger liquefies and cools the natural gas to the required LNG storage condition of about −119.4 °C and 11.45 bar pressure. Subsequent expansion prepares the LNG for the CCC process. The streams labeled “From CCC” and “Water” return to the liquefaction process from the CCC process. Water can be used to reduce heat load but, as will be shown in the transient analysis, a separate heat exchanger for water is more robust. Table 3 summarizes the optimized mixed refrigerant composition and key parameters, where ER, B and ES represent energy storing, balanced, and energy recovery, respectively, that is, conditions when LNG is accumulating for future use by the CCC process, when LNG demand from the CCC process is balanced with its production rate, and when stored LNG levels are dropping.

### 3.3. Phase equilibrium equations

Phase equilibrium provides the quantitative basis for much of the process simulation. The Peng–Robinson equation is used in this study. The PR equation is a cubic equation of state:

$$P = \frac{RT}{v-b} - \frac{a}{v(v+b)+b(v-b)} \tag{1}$$

where:

$$a = \sum\sum z_i z_j (a_i a_j)^{0.5}(1-k_{ij}) \tag{2}$$

$$b = \sum z_i b_j \tag{3}$$

The PR equation can also be expressed in the form of a compression compressibility factor, in which form its classification as a cubic equation of state is more evident (cubic in compressibility):

$$Z^3 - (1-B)Z^2 + \left(A - 3B^2 - 2B\right)Z - \left(AB - B^2 - B^3\right) = 0 \tag{4}$$

where:

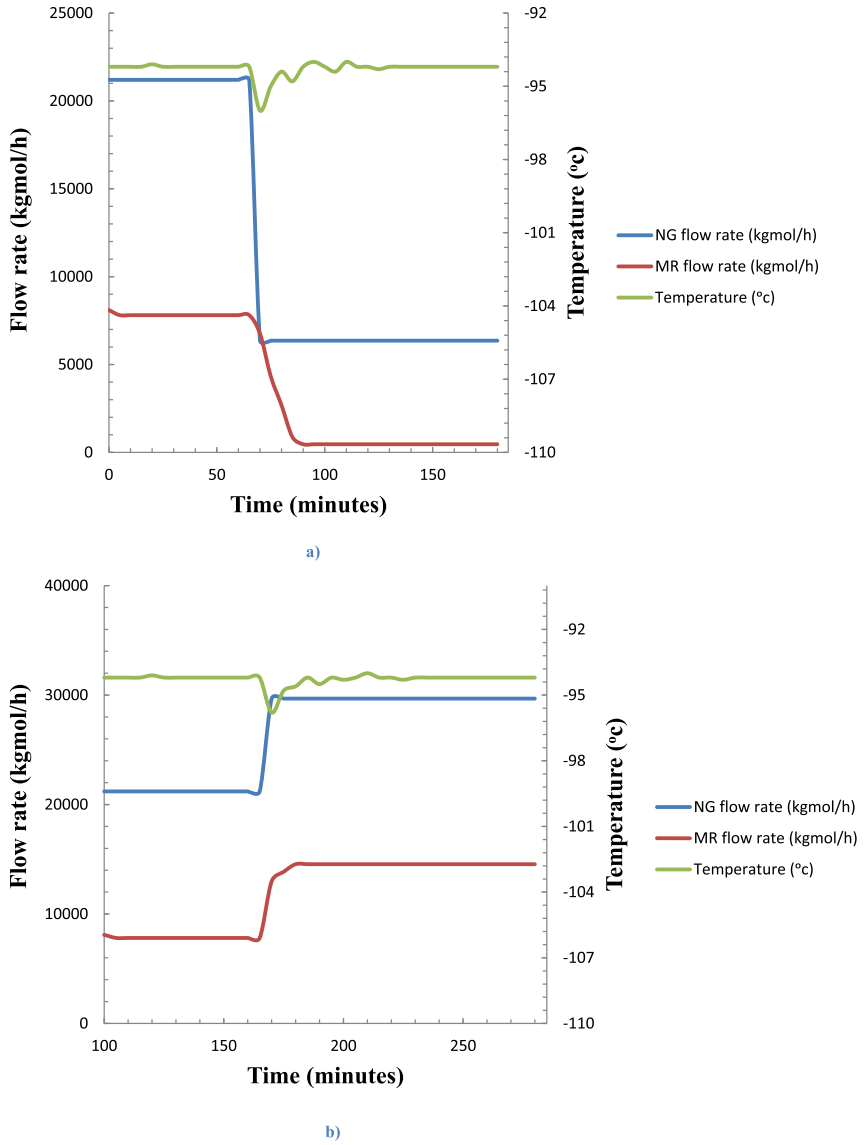


**Fig. 6.** Output LNG temperature and NG and MR flow rates in a) B-ER, b) B-ES.

$$Z = \frac{PV}{RT} \tag{5}$$

$$A = \frac{aP}{(RT)^2} \tag{6}$$

$$B = \frac{bP}{RT} \tag{7}$$

### 3.4. Heat exchanger's efficiency

The technical literature does not define a heat exchanger efficiency. This document suggests one such useful definition. Insulated heat exchangers conserve enthalpy, so a first-law definition is problematic. That is, the enthalpy flowing out of the system equals that flowing in. Heat exchangers do not involve shaft work, so a second-law definition (work over heat) does not naturally come to mind. Nevertheless, this document proposes a second-law definition for heat exchanger efficiency that is both useful and simple [19].

Conceptually, this efficiency describes the consequence of heat exchange on the flow streams' (a) ability to do work (availability or exergy) or, equivalently, (b) entropy. Quantitatively, the heat exchanger efficiency is one minus the difference in exergy between the streams exiting and entering a heat exchanger normalized by the largest achievable difference in such exergy. The largest achievable difference with respect to heat exchange occurs if all the streams come to the same temperature. These analyses and this definition assume no heat transfer between the exchanger and its surroundings. Therefore, the difference in exergy is proportional to a difference in entropy, with the ambient temperature as a proportionality constant. This expression depends on conditions at thermal equilibrium, that is, at the temperature the streams would become if the inlet streams were to equilibrate at a single temperature

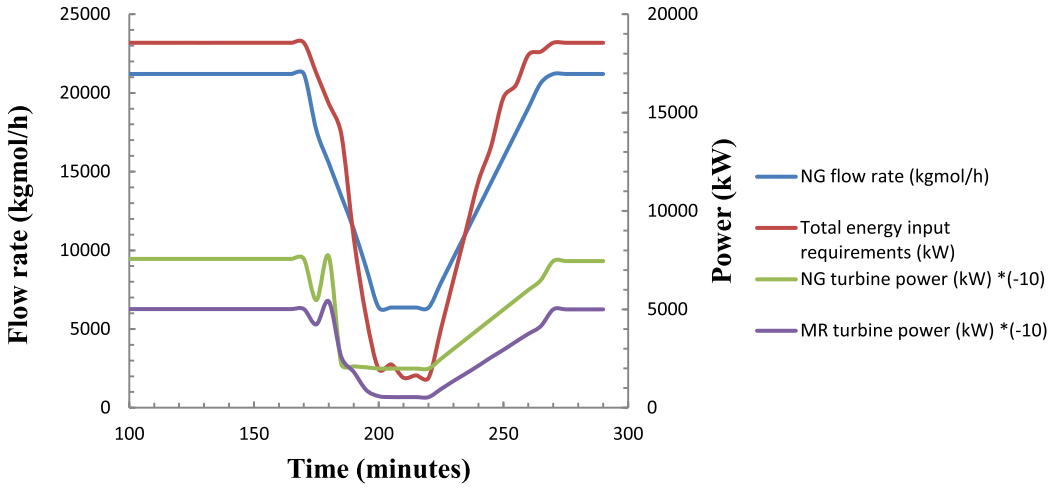


a)

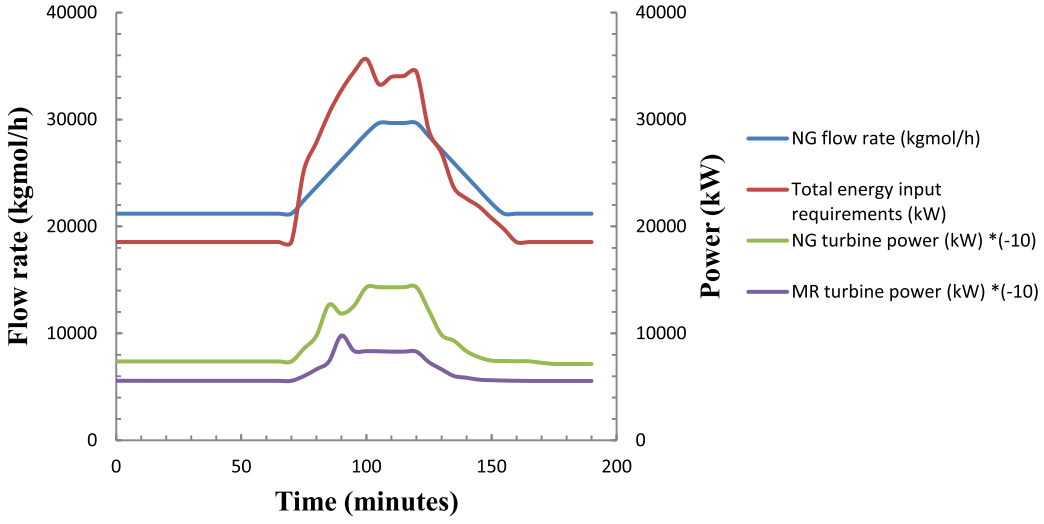


b)

**Fig. 7.** Ramping a) B-ER-B and b) B-ES-B performances.

$$\eta = 1 - \frac{\sum_{outlet} m_i \hat{b}_i - \sum_{inlet} m_i \hat{b}_i}{\sum_{eq} m_i \hat{b}_i - \sum_{inlet} m_i \hat{b}_i} = 1 - \frac{\Delta_{obs} m_i \hat{s}_i}{\Delta_{eq} m_i \hat{s}_i} = \frac{\sum_{eq} m_i \hat{s}_i - \sum_{outlet} m_i \hat{s}_i}{\sum_{eq} m_i \hat{s}_i - \sum_{inlet} m_i \hat{s}_i} \quad (8)$$

where $\hat{b}_i = \hat{h}_i - T_0 \hat{s}_i$ represents the specific exergy of stream $i$ and $\Delta_{eq} m_i \hat{s}_i$ is the difference between the entropy in all the streams at equilibrium temperature and entropy of the streams at the inlet temperature. The temperature $T_0$ represents the temperature of the ambient environment and, since it drops out of the equation, is irrelevant to the exchanger efficiency. This ambient temperature should not affect a well-posited efficiency definition for reasons discussed below. The middle form of the equation results from the sum of the inlet enthalpy flows equaling the sum of the outlet enthalpy flows.

This efficiency becomes unity if the total exergy of the outlet streams equals that of the inlet streams, which can only occur in the limit of the hot and cold streams transferring heat with no temperature difference at any given point along the exchanger (ideal heat exchanger). The efficiency is zero if all outlet streams approach the same equilibrium temperature, which represents the poorest possible heat exchanger performance from an efficiency or entropy standpoint. An efficiency of 50% indicates that heat exchanger generates half of much entropy it would generate if all streams come to the same temperature.

### 3.5. Transient modeling

#### 3.5.1. Dynamic heat exchanger modeling

Developing a dynamic model of the heat exchanger represents arguably the most critical aspect of this analysis.

Accurate equipment sizing, proper pressure or flow rate specifications as boundary conditions and specifying resistance of unit operations are needed for dynamic simulation of the plant. Geometry information is important since transient behaviors are

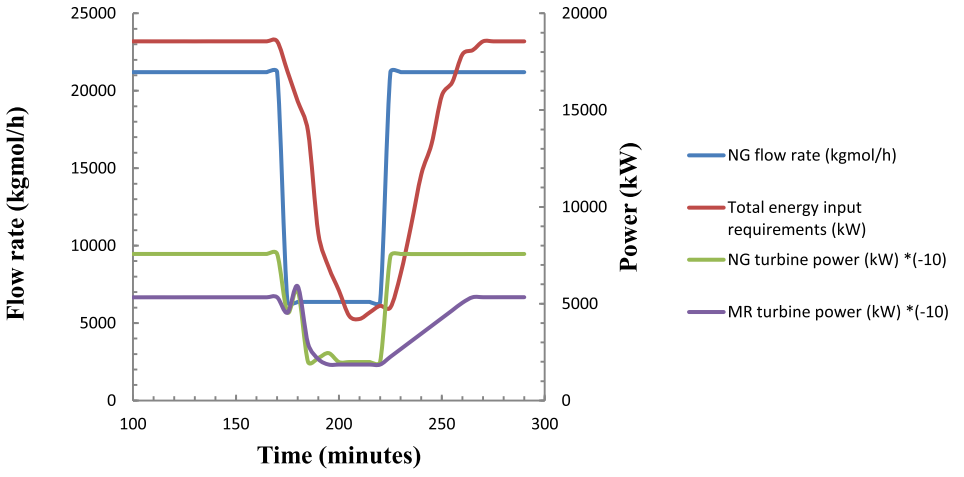


a)

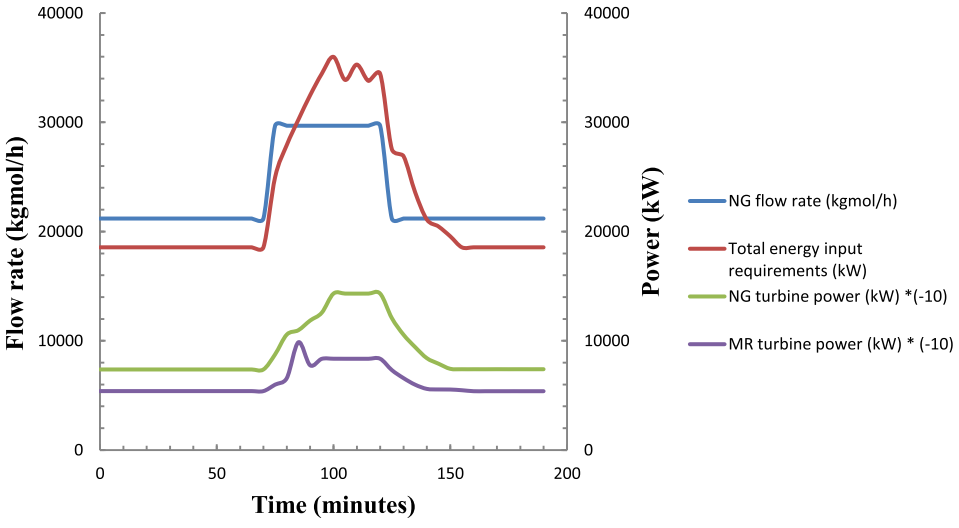


b)

**Fig. 8.** Step changing a) B-ER-B and b) B-ES-B performance.

influenced by volume of equipment. Rating of a multi-stream plate-frame type heat exchanger includes:

a) Length and width of the exchanger
b) Layer configuration
c) Zone configuration
d) Heat transfer configuration.

*3.5.1.1. Length and width of the exchanger.* By using Aspen economic analysis in HYSYS, total surface area is achievable. Considering number of zones, the surface area for each zone and layer can be calculated.

*3.5.1.2. Layer configurations.* The configuration of heat exchanger streams affects the total heat load distribution. An optimal configuration involves alternating cold and hot layers with a countercurrent flow pattern.

*3.5.1.3. Zone configuration.* In a pressure-flow dynamic model, the heat exchanger determines flowrates using resistance equations. Each zone features a stacking pattern with one feed and one product connected to each representative layer in the pattern. The resistance equation modeled after turbulent flow equation is:

$$F = k\sqrt{\rho \times \Delta P} \tag{9}$$

where:

$k$ = pressure flow coefficient, $\frac{kg}{h} \times \sqrt{\frac{\frac{kg}{m^3}}{kPa}}$
$\rho$ = density of fluid, $kg/m^3$
$\Delta P$ = total pressure drop, $kPa$

The resistance equation calculates flowrates from the pressure differences of the surrounding nodes using pre-specified k-values.

The dynamic heat exchanger requires k-values. However, the temperature and pressure drop for each zone are not determined, thus exact k-values cannot be specified. The temperature and pressure differences in dynamic mode provide k-value estimates. K-value computation is one of the most important steps for

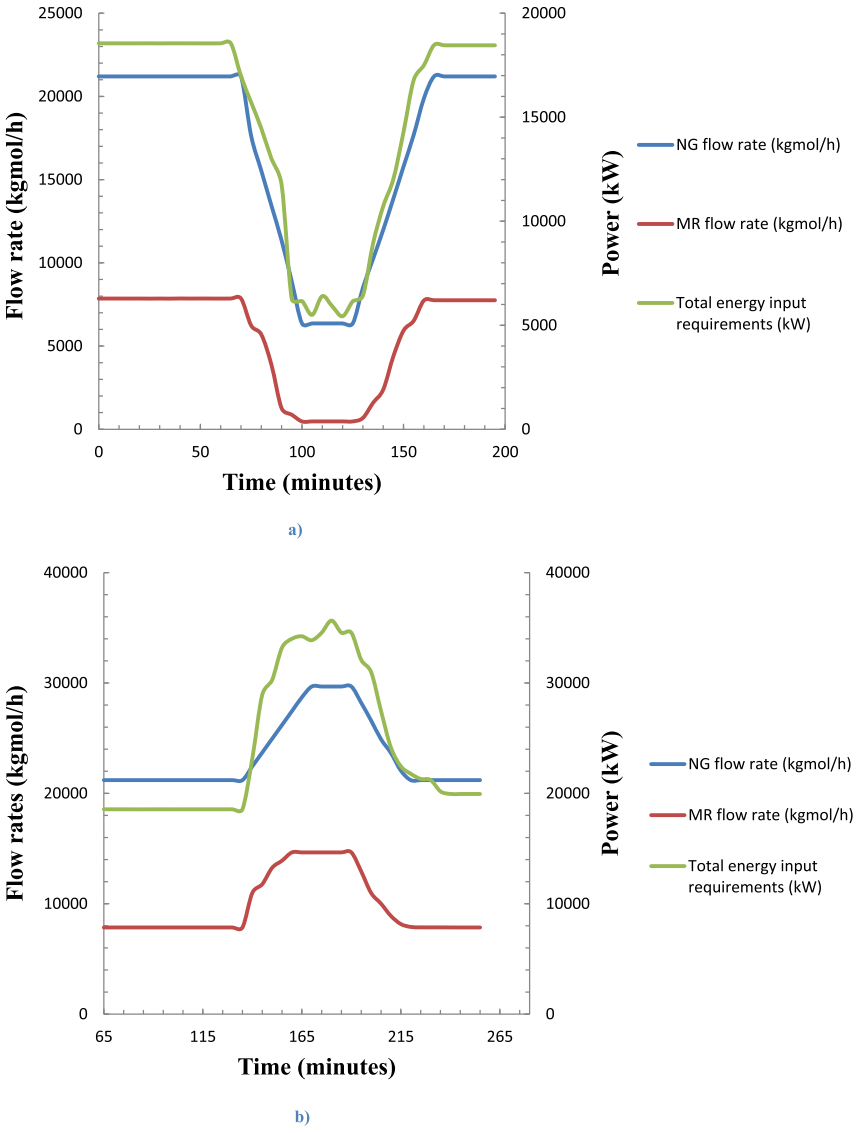


**Fig. 9.** Change of MR and NG flow rates versus total energy input requirements with ramping a) B-ER-B and b) B-ES-B.

dynamic heat exchangers' design. Improper specification produces unbalanced pressures and flow rates in our streams in transient.

*3.5.1.4. Heat transfer configuration.* The combined area and heat transfer coefficient, UA, determines the convective heat transfer between the steam and the metal that surrounds it. Aspen HYSYS provides UA values for each stream. Knowing the surface areas determines the heat transfer coefficient, U, for each layer. Aspen Economic Analysis helps provide surface areas (A). Equal UA-values are fixed for each zone. Initial values can be estimated from steady-state UA values.

## 4. Results and discussion

### 4.1. Process optimization

To optimize a cryogenic heat exchanger, a sensitivity analysis was performed in Aspen to achieve predefined outlet conditions of natural gas. The optimization is essentially a non-automated version of the genetic algorithm. Several variables provide the optimization objective function for the mixed refrigerant stream, including pressure, composition, and flow rate along with the pressure exiting the expansion turbine. For purposes of optimization, the composition and flow rate were tied together so that flow rates of individual components were specified rather than mole percent and overall flow rate. The mixed refrigerant was comprised of hydrocarbons $C_1$–$C_5$ (with $C_4$ and $C_5$ being n-variations instead of iso-variations) leading to a total of 7 variables once a fixed natural gas condition was specified. Each of these variables had 3–5 values, including the then current value and at least one lower and higher value. The decision to include additional higher and/or lower values is made based on the previous set of variables. Aspen's sensitivity analysis tool allows calculation of the total power required by the cooling loop. Because of the large number of possible combinations, each value was usually only given 3 values unless more were expected to significantly speed up the process. The algorithm selects a new solution based on the two previous best solutions and the process was repeated until the optimal solution repeated several times with adjustments to input values. The work done per unit of LNG production formed the objective function:

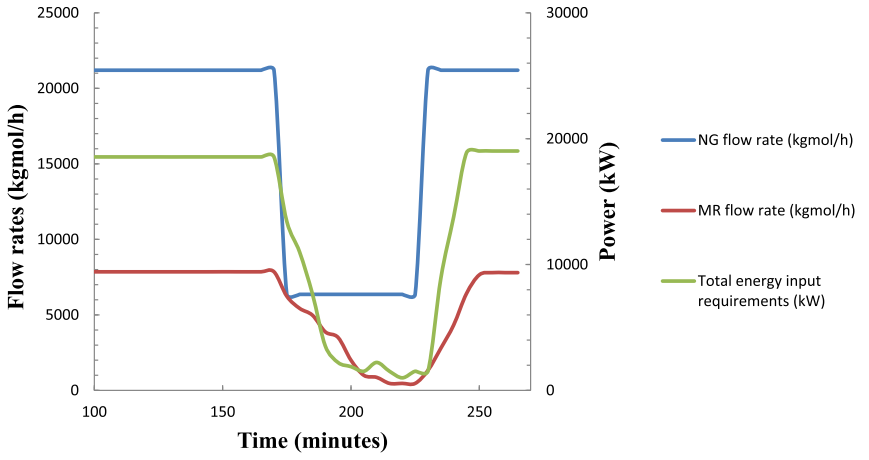


a)

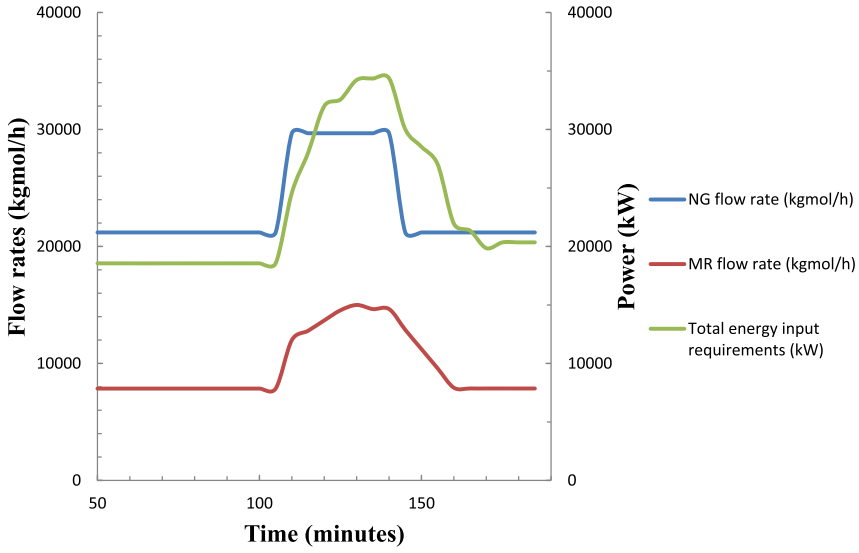


b)

**Fig. 10.** Change of MR and NG flow rates versus total energy input requirements with step size change a) B-ER-B and b) B-ES-B.

$$f(X) = \min\left(\frac{W_{net}}{q_{LNG}}\right) \tag{10}$$

where:

$$W_{net} = \sum W_{compressors} - \sum W_{expanders} \tag{11}$$

$q_{LNG}$ represents the mass flow of the produced LNG.

The model assumed that:

1) A minimum of 1 °C approach temperature was necessary in brazed plate heat exchangers,
2) Compressors operate at 92% isentropic efficiencies,
3) Inter- and after-coolers are capable of cooling the gases to 20 °C
4) No condensates formed in the compressors (100% vapor flow)
5) A single liquid phase forms in the turbines and pumps (100% liquid flow)
6) The sum of mixed refrigerant mole/mass fraction is 1
7) The expansion valves operate adiabatically

The optimized model yielded energy input requirements is illustrated by Table 4:

### 4.2. Exergy analysis methodology

Li et al. [20] have introduced the exergy losses equations of the equipment (see Table 5). Table 6 summarizes the exergy changes associated with this process. Fig. 3a–c particularly show the exergy losses for major equipment in three cases. In a normal liquefaction process, the exergy losses of the water coolers are very large because the outlet temperature of the compressor is high; therefore it loses large amounts of exergy when the gas is cooled down to a low temperature.

And the total exergy loss is given in Table 6:

The compressors contribute small exergy losses [17,21] in the process because compression ratios are generally small. This can be

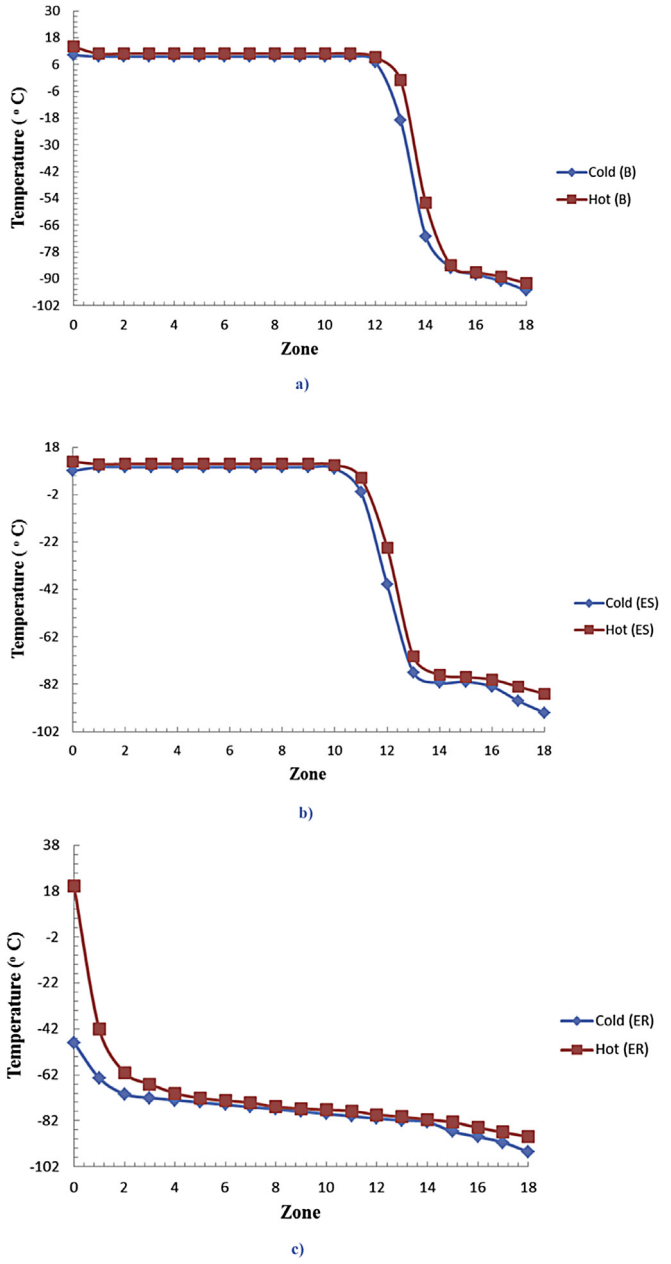


**Fig. 11.** Temperature profiles for a) B, b) ES and c) ER cases.

improved by high efficiency, multi-stage, intercooled compression. The valves contribute less than 0.1% to the total exergy loss.

Exergy losses are lower in these heat exchangers than those reported in literature [9,17,21], primarily because of the returning flow. The temperature profiles are also consistent with these high efficiencies.

### 4.3. Efficiency results for heat exchanger

Heat exchanger's efficiency would be in Table 7:

In this study we try to keep our transient heat exchanger's efficiency high and stable like steady-state values.

### 4.4. Transient modeling of natural gas liquefaction process

Fig. 4 shows the process flow diagram of natural gas liquefaction process using a mixed refrigerant.

Aspen HYSYS provides dynamic modeling of this process, which required several modifications relative to the steady-state model. Some of the most important include:

1) PID (proportional–integral–derivative) controller: Heat exchanger outlet temperatures are controlled by changing mixed refrigerant flow rates.
2) Digital on/off controllers are one of the most basic forms of regulatory control and are used, for example, for water flow rate. Water flow rate differs for every case. When the digital controller detects that natural gas flow rate is below the set point, the element turns on and when the natural gas raises the set point, the element turns off.
3) Transfer functions have two important impacts on our project. One is when we want to break closed recirculation loops, which are very difficult to converge in steady state and far more difficult in transient models. For instance if a recirculation loop breaks into an open loop, the input and the output of this loop should have the same conditions, including pressure, temperature and flow rate. Transfer functions make these parameters the same. The second impact is ramping. Transfer functions provide some random variations in flows that help establish the robustness of the model.

As shown in Fig. 5a–c, in all three case PID controllers reaches the set point and satisfy the output temperature. It takes 2–8 min for a PID to reach the set point in three cases. The set point temperature is −94 °C before NG expansion.

The output temperature for LNG and MR and NG flowrates appear in Fig. 6a and b. Changing NG flowrate (decreasing or increasing) leads to changes in MR flow rate to maintain a constant set point temperature.

The model explored responses to both step changes and ramping changes in flow rate. During a step change, the natural gas flow rate varied among three specific values, one each for energy storing, balanced, and energy recovery. This discussion focuses on four main transient responses during these changes, including total energy usage, NG turbine production, MR turbine production and NG flow rate (Figs. 7a, b, 8a and b). These responses adequately provide the behavior required to balance changing power availability (Fig. 1).

Total energy usage decreases as NG flow decreases and vice versa. Energy productions by NG and MR turbines increase as NG flow decreases.

The changes in flow rate versus total energy consumption appear in Figs. 9a, b, 10a and b. NG and total energy input requirements decrease and increase together because the process MR requirements scale approximately with NG flow rate, with some variation due to changes in process equipment temperature profiles.

Heat exchanger temperature profiles represent the most critical component of these simulations, both because of entropy generation and because of thermal stresses. Temperature profiles vary both spatially and temporally, making them difficult to illustrate in a single graph. The previous graphs provide some idea of the temporal variation as the transients in these graphs largely arise from changes in the heat exchanger profiles. The end-point spatial variations in the heat exchanger temperatures appear in Fig. 11a–c, all of which are computed as the final profile after then step change in flow rate. As indicated, all of the heat exchangers come to a their optimal condition of small and approximately constant temperature differences between the hot and cold streams even though the profiles are far from linear. However, the temperature changes at any one location as the process moves between ER, B, and ES modes can be large enough that significant

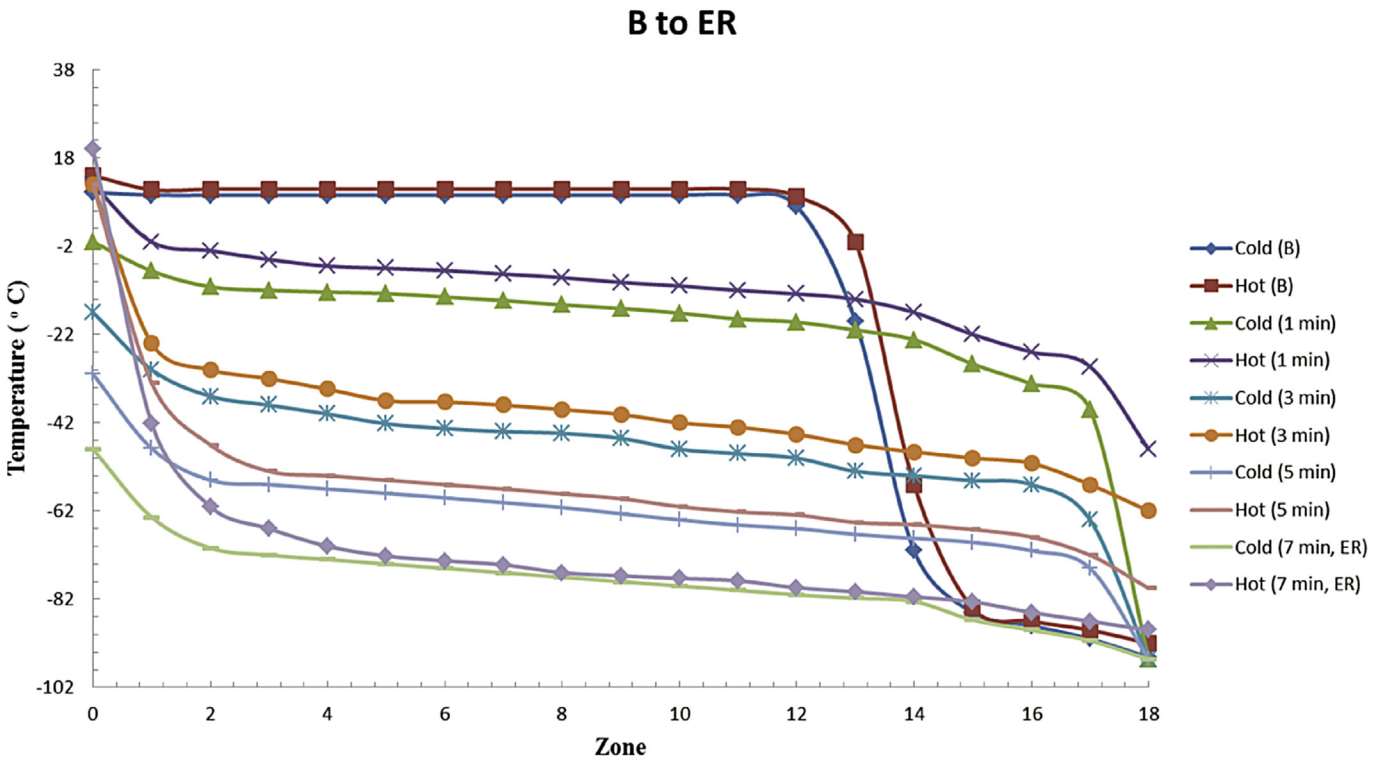


**Fig. 12.** Transient temperature profiles in moving from the B to the ER condition. After 7 min, the transition is essentially complete.

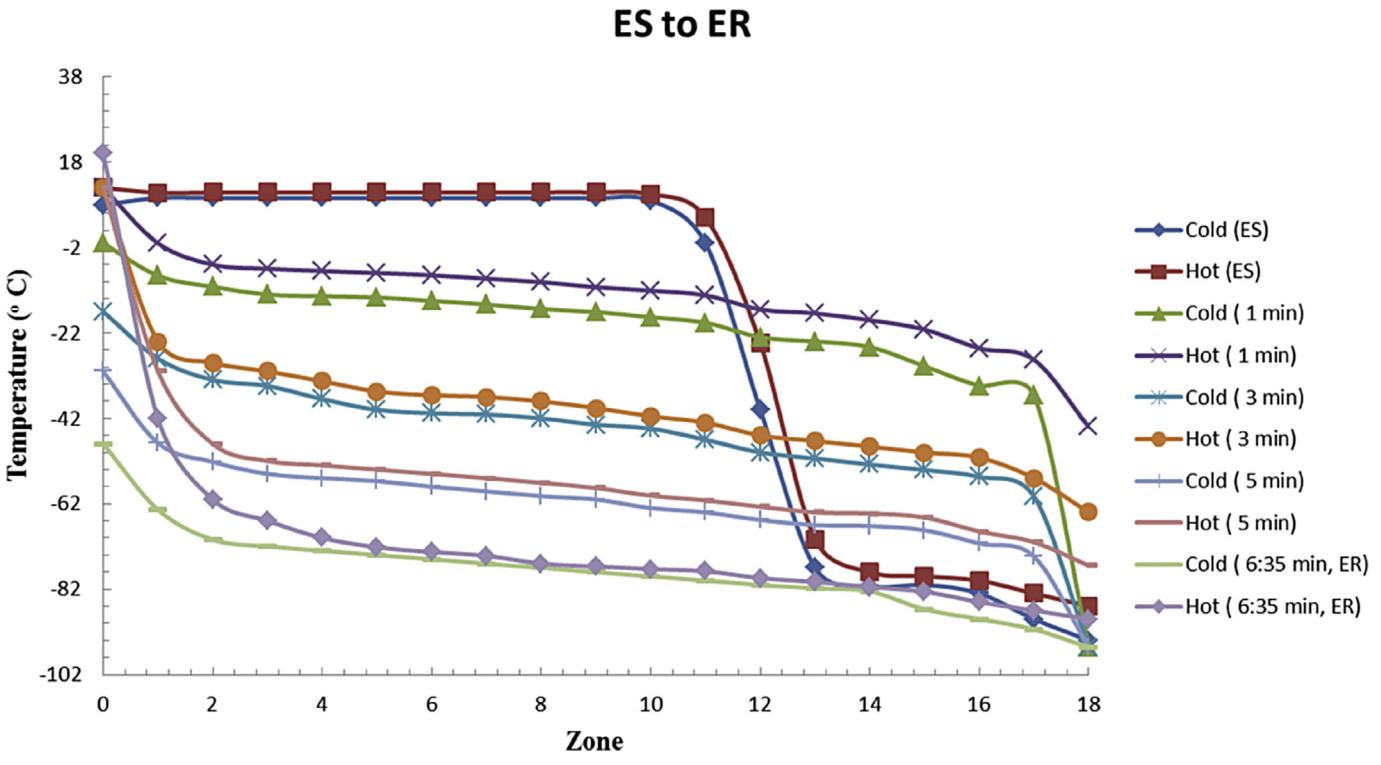


**Fig. 13.** Transient heat exchanger temperature profiles in moving from the ES to the ER condition. After 6 min and 35 s, the transition is essentially complete.

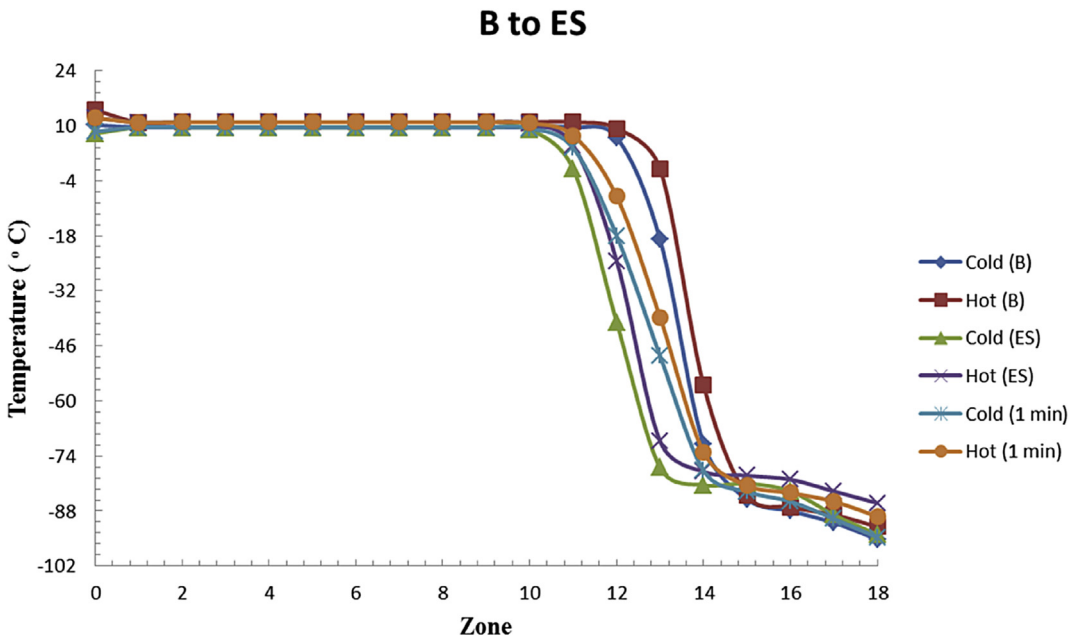


**Fig. 14.** Transient heat exchanger temperature profiles in moving from ES to the B conditions. After 2 min and 54 s, the transition is essentially complete.

thermal stresses will arise if the rate of these changes is not carefully managed.

These transient temperature profiles created in moving from B to ER modes, ES to ER modes, and B to ES conditions appear in Figs. 12–14, respectively. As illustrated, in moving through these transitions, the internal temperatures change over a large range in a short amount of time. Depending on heat exchanger construction and operation details, these changes could exceed the allowable temperature stress limits of the heat exchangers. Recent technological innovations provide means of greatly reducing or eliminating these stresses. However, in traditional designs, these stresses can limit the response times of the entire system.

### 4.5. Transient efficiency

The transient heat exchanger efficiency decreases as temperature differences between streams increase. While the previous results show that these differences can be small once the heat exchangers adjust to their new temperature profiles, it is not possible to maintain these narrow temperature differences as profiles change. The thermal heat transfer efficiency conceptually represents the Gibbs energy/entropy/exergy change in the system, as explained in Section 3.4. Fig. 15 illustrates these changes as a function of time for rapid changes in flow rates. The process initially responds almost instantly and reaches a new quasi-steady value in about 3 min. However, these response times are limited only by the transient heating of the mainly the heat exchangers. In practice, the limit of temperature change rates in heat exchangers is about 1 °C per minute to avoid excessive thermal stresses. At this rate, these transients would require about 20 min of operating time to adjust to the new conditions. Efficiencies greater than 100% indicate that the heat exchanger structural elements are helping to change a fluid temperature in addition to the counter-flowing fluid.

## 5. Conclusions

This investigation explores Aspen HYSYS models and optimizations for a natural gas liquefaction process that provides coolant for the energy-storing version of the CCC (cryogenic carbon capture™) process. The steady-state version of the process provides baseline information such as exergy losses and efficiencies. Process simulation for three cases provided a basis for comparison:

- Energy storing, where LNG production increases by 40% to use excess energy available on the grid,
- Balanced, where LNG production equals LNG demand from the power plant to run the CCC process, and
- Energy recovery, where LNG production decreased by 70% to decrease the parasitic loss and hence place more power on the grid when demand is high.

The SMR process provides the most efficient overall design. During energy storage, energy demand increases significantly compared to the other states since excess LNG is produced. This operating mode most closely resembles traditional LNG production. During energy recovery, the energy demand decreases relative to the other states since stored LNG supplements the amount produced from this process and heat integration from the excess LNG decreases energy consumption. Heat exchanger efficiencies in all three cases remain nearly constant except for short transients. Exergy analysis has been studied for major equipment in this process and indicates the importance of high efficiency for heat exchangers. Transient techniques for modeling include K-values, U-values, zone configuration and heat transfer rating. Optimum energy input requirements of 0.0083 kW/kg NG for ER, 0.0613 kW/kg NG for B and 0.0706 kW/kg NG for ES have been obtained. Highest efficiencies of 93.86% for B, 80.21% for ES and 74.35% for ER have been achieved. Exergy losses of 1%, 2% and 13% for heat exchanger in three cases confirm the high efficiency for this unit. PID controller has been tuned perfectly so that it takes 2–7 min for MR flow and heat exchanger to reach the required set points. As illustrated, in moving through transitions, the internal temperatures change over a large range in a short amount of time. Depending on heat exchanger construction and operation details, these changes could exceed the allowable temperature stress limits of the heat exchangers. Heat exchanger has constant transient efficiency of 78–82%.Transient responses in case of ramping and step changes

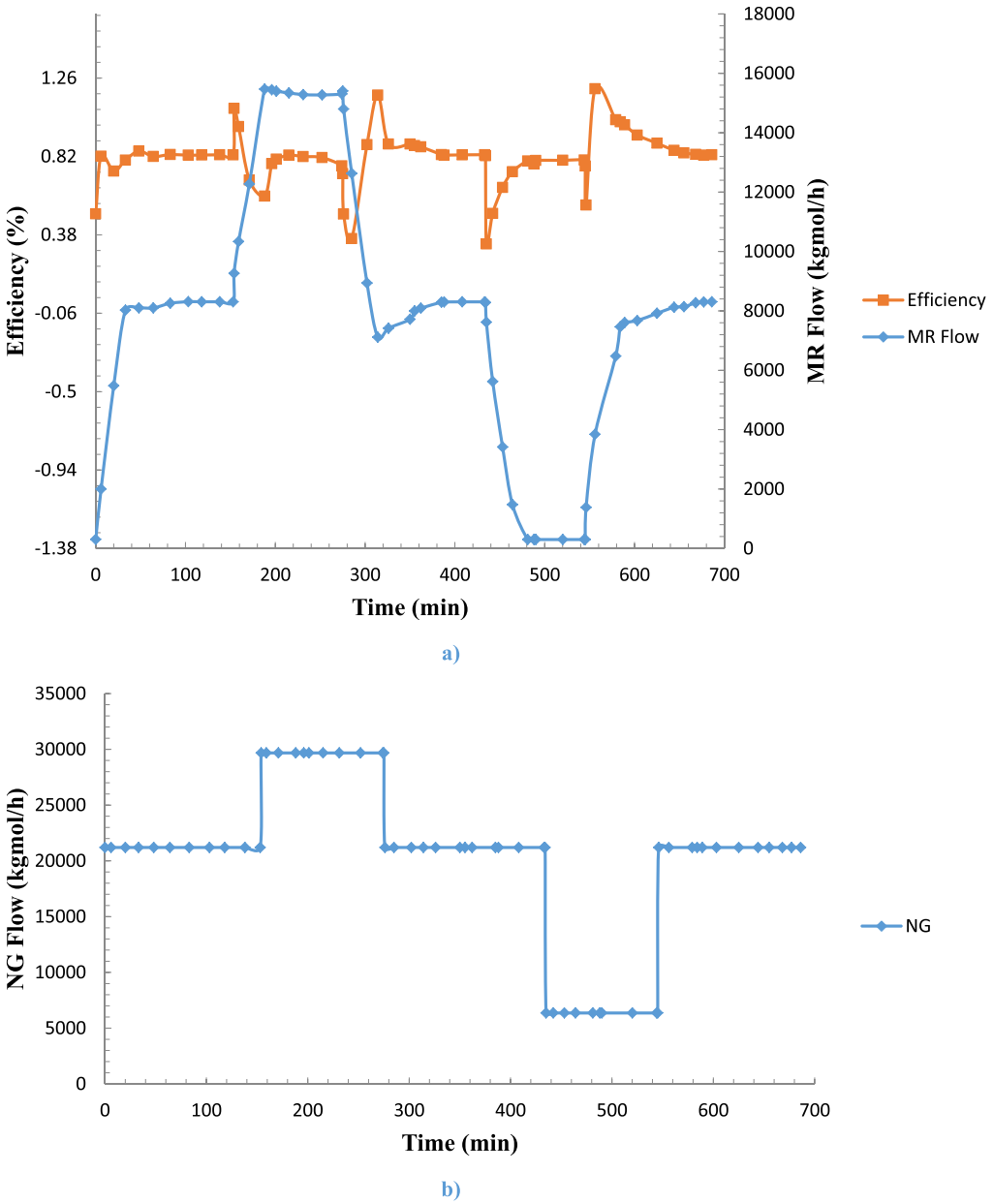


**Fig. 15.** Transient efficiency with respect to a) MR and b) NG flow rates.

indicate typical system responses to changes in load. Temperature profiles illustrate low exergy losses for heat exchanger after their internal temperature profiles adjust to the new flow rates. Transient efficiencies of the heat exchangers indicate that heat exchanger efficiencies vary considerably as the internal temperature profiles adjust.

## Acknowledgments

The financial and technical support of Sustainable Energy Solutions (SES) LLC of Orem, Utah, the Advanced Research Projects Agency – Energy (ARPA-E), U.S. Department of Energy, under Award Number DE-AR0000101 is gratefully acknowledged. This project was partially funded by SES projects sponsored by Advanced Conversion Technologies Task Force in Laramie, Wyoming through the School of Energy Resources and by the Climate Change and Emissions Management Corporation (CCEMC) of Alberta, Canada CCEMC.

## References

[1] Kumar S, Kwon HT, Choi KH, Cho JH, Lim W, Moon I. Current status and future projections of LNG demand and supplies: a global prospective. Energy Policy 2011;39:4097–104.
[2] Shariq Khan M, Lee M. Design optimization of single mixed refrigerant natural gas liquefaction process. Energy 2013;49:146–55.
[3] He T, Ju Y. Optimal synthesis of expansion liquefaction cycle for distributed-scale LNG (liquefied natural gas) plant. Energy 2015;88:268–80.
[4] Khan MS, Karimi IA, Bahadori A, Lee M. Sequential coordinate random search for optimal operation of LNG (liquefied natural gas) plant. Energy 2016;89:757–67.
[5] He TB, Ju YL. A novel process for small-scale pipeline natural gas liquefaction. Appl Energy 2014;115:17–24.
[6] Remeljej CW, Hoadley AFA. An exergy analysis of small-scale liquefied natural gas (LNG) liquefaction processes. Energy 2006;31:2005–19.
[7] Gu A, Lu X, Wang R, Shi Y, Lin W. Liquefied natural gas technology. China Machine Press; 2004.

[8] Cao WS, Lu XS, Lin WS, Gu AZ. Parameter comparison of two small-scale natural gas liquefaction processes in skid-mounted packages. Appl Therm Eng 2006;26:898–904.
[9] Shirazi MMH, Mowla D. Energy optimization for liquefaction process of natural gas in peak shaving plant. Energy 2010;35:2878–85.
[10] Yoshitugi K, Moritaka N. Development of liquefaction process for natural gas. J Chem Eng Jpn 1997;30:626–30.
[11] Van de Graaf J, Pek B. The Shell parallel mixed refrigerant process. USA instrumentation & processing. 2005.
[12] Safdarnejad SM, Hedengren JD, Baxter LL. Plant-level dynamic optimization of cryogenic carbon capture with conventional and renewable power sources. Appl Energy 2015;149:354–66.
[13] Baxter L, System and methods for integrated energy and cryogenic carbon capture. Patent WO 2013062922 A1, 2013.
[14] Fazlollahi F, Bown A, Ebrahimzadeh E, Baxter LL. Design and analysis of the natural gas liquefaction optimization process- Energy Storage of Cryogenic Carbon Capture (CCC-ES). Energy 2015;90:244–57.
[15] Yang YM, Kim JH, Seo HS, Lee K, Yoon IS. Development of the world's largest above-ground full containment LNG storage tank. In: Amsterdam: 23rd World Gas Conference; 2006.
[16] Wise JJ. Base load and peaking economics and the resulting adoption of carbon dioxide capture and storage system for electric power plants. In: 7th International Conference on Greenhouse Gas. College Park, MD: Pacific Northwest National Laboratory and Joint Global Change Research Institute; 2004.
[17] Yuan Z, Cui M, Xie M, Li C. Design and analysis of a small-scale natural gas liquefaction process adopting single nitrogen expansion with carbon dioxide pre-cooling. Appl Therm Eng 2014;64:139–46.
[18] Jensen MJ, Russell CS, Bergeson D, Hoeger CD, Frankman DJ, Bence CS, et al. Prediction and validation of external cooling loop cryogenic carbon capture (CCC ECL) for full-scale coal-fired power plant retrofit. Int J Greenh Gas Control 2015;42:200–12.
[19] Ebrahimzadeh E, Wilding P, Frankman D, Fazlollahi F, Baxter LL. Theoretical and experimental analysis of dynamic plate heat exchanger: non-retrofit configuration. Appl Therm Eng 2015;93:1006–19.
[20] Li QY, Ju YL. Design and analysis of liquefaction process for offshore associated gas resources. Appl Therm Eng 2010;30:2518–25.
[21] He TB, Ju YL. Design and optimization of natural gas liquefaction process by utilizing gas pipeline pressure energy. Appl Therm Eng 2013;57:1–6.